Sensing earth's rotation with a helium–neon ring laser operating at 1.15 μm

Article *in* Optics Letters · April 2015

DOI: 10.1364/OL.40.001705

CITATIONS
18

READS
133

7 authors, including:

K. Ulrich Schreiber
Technische Universität München
288 PUBLICATIONS **4,540** CITATIONS
SEE PROFILE

Robert J Thirkettle
University of Canterbury
12 PUBLICATIONS **189** CITATIONS
SEE PROFILE

Robert Hurst
University of Canterbury
22 PUBLICATIONS **456** CITATIONS
SEE PROFILE

David Follman
Thorlabs, Inc.
77 PUBLICATIONS **968** CITATIONS
SEE PROFILE

Sensing earth's rotation with a helium–neon ring laser operating at 1.15 μm

K. Ulrich Schreiber,[1,*] Robert J. Thirkettle,[2] Robert B. Hurst,[2] David Follman,[3] Garrett D. Cole,[3,4] Markus Aspelmeyer,[5] and Jon-Paul R. Wells[6]

[1]*Technische Universitaet Muenchen, Forschungseinrichtung Satellitengeodaesie, Geodaetisches Observatorium Wettzell, 93444 Bad Kötzting, Germany*

[2]*Department of Physics and Astronomy, University of Canterbury, Private Bag 4800, Christchurch 8020, New Zealand*

[3]*Crystalline Mirror Solutions LLC, 114 E Haley, Suite N, Santa Barbara, California 93101, USA*

[4]*Crystalline Mirror Solutions GmbH, Seestadtstr. 27, Top 1.05, A-1220 Vienna, Austria*

[5]*Vienna Center for Quantum Science and Technology (VCQ), Faculty of Physics, Univ. of Vienna, A-1090 Vienna, Austria*

[6]*The Dodd-Walls Centre for Photonic and Quantum Technologies and Department of Physics and Astronomy, University of Canterbury, Private Bag 4800, Christchurch 8020, New Zealand*

**Corresponding author: schreiber@fs.wettzell.de*

Received February 13, 2015; revised March 8, 2015; accepted March 13, 2015; posted March 16, 2015 (Doc. ID 234633); published April 8, 2015

We report on the operation of a 2.56 m^2 helium–neon based ring laser interferometer at a wavelength of 1.152276 μm using crystalline coated intracavity supermirrors. This work represents the first implementation of crystalline coatings in an active laser system and expands the core application area of these low-thermal-noise cavity end mirrors to inertial sensing systems. Stable gyroscopic behavior can only be obtained with the addition of helium to the gain medium as this quenches the 1.152502 μm ($2s_4 \rightarrow 2p_7$) transition of the neon doublet which otherwise gives rise to mode competition. For the first time at this wavelength, the ring laser is observed to readily unlock on the bias provided by the earth's rotation alone, yielding a Sagnac frequency of approximately 59 Hz.

OCIS codes: (120.5790) Sagnac effect; (140.3370) Laser gyroscopes; (140.3560) Lasers, ring.
http://dx.doi.org/10.1364/OL.40.001705

The first demonstration of rotation sensing with a ring laser gyroscope was performed by Macek and Davies in 1963 using a 1 m^2 helium–neon laser system operating at a wavelength of 1.153 μm [1], just two years after the first report of laser oscillation in a helium–neon discharge [2]. Their device utilized four gain tubes, one in each of the sides of the square ring and, therefore, had a total of 20 intracavity surfaces. Rotation sensing was attained through an externally imposed rotation via a mechanical turntable.

Over the last two and a half decades, large ring laser gyroscopes have increased in size from approximately 1 m^2 to over 800 m^2 [3,4]. The reason for this is obvious from Eq. (1) for laser gyroscopes, which relates the beat frequency δf of the two counter propagating continuous wave (CW) laser beams inside the ring cavity to the rate of rotation (Ω) imposed upon the projection on the normal vector ($\mathbf{n}$) of the ring laser structure [5,6]:

$$\delta f = \frac{4A}{\lambda P}\mathbf{n}\cdot\Omega. \tag{1}$$

Thus, it is clear that increasing the perimeter (P) of the device and, therefore, the area (A) enclosed by the two laser beams leads to an increased sensor resolution. Currently the highest usable sensitivity of 1×10^{-8} of the earth's rotation rate (Ω_E) is achieved by the German Gross ring [7]. Ring lasers are now poised for realistic attempts at terrestrial measurement of general relativistic phenomena, such as the Lense–Thirring effect [8].

At some level of performance, all ring laser gyroscopes are limited by geometrical instabilities, which manifest themselves in the measurement quantity (δf) through the backscatter process. Backscatter arises from scattering of the intracavity laser beams into the counter propagating beam path, inducing both phase and optical frequency variations to that beam. Geometric instabilities cause time-varying optical frequency fluctuations, which are transferred to the Sagnac frequency as a time-varying readout error superimposed on the signal from earth's rotation. In our gas lasers, the only intracavity elements are the supermirrors which form the cavity itself and, therefore, it is mirror imperfections that drive the backscatter process. One approach to minimize the influence of backscatter is to utilize longer wavelength laser radiation since the backscatter amplitude will decrease dramatically, in the limit of Rayleigh scattering proportional to the reciprocal of the fourth power of the laser wavelength [9]. The downside of such an approach is an unavoidable reduction in the scale factor of the gyroscope. In principle, however, a net improvement in performance can be expected.

The supermirrors employed in this experiment consist of 8 mm diameter crystalline coatings transferred to super-polished fused silica substrates with a 4 m radius of curvature (ROC). As in a previous demonstration of an ultrastable optical reference cavity [10], these mirrors are produced via a microfabrication-based substrate-transfer technique, whereby a single-crystal Bragg mirror is initially grown on a lattice-matched GaAs wafer by molecular beam epitaxy (MBE), selectively removed from this initial growth template using a series of lithography and etching steps, and is then bonded to the final optic [Fig. 1 (inset)]. Such mirrors have the additional advantage of minimizing thermally induced mechanical fluctuations in the mirror coatings. This is unlike the industry standard ion beam sputtered dielectric multilayer mirrors

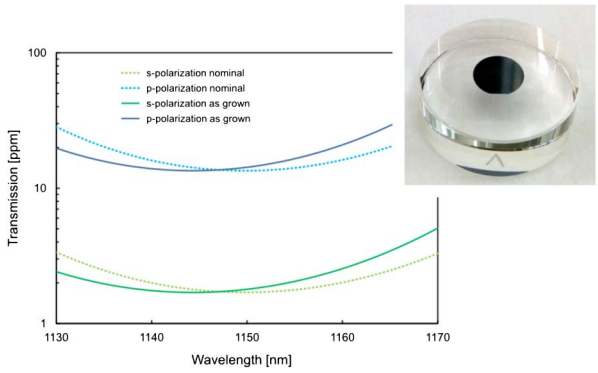

Fig. 1. Details of the crystalline supermirrors. The plot shows the transmission spectrum for the ideal design and as-grown multilayer under illumination at a 45° angle of incidence. The inset includes a photograph of a completed mirror structure consisting of an 8 mm diameter GaAs/AlGaAs mirror pad transferred to a 25 mm diameter fused silica substrate. The small flat on the coating disc indicates the crystal orientation, in this case parallel to the ⟨110⟩ direction.

used in all previous ring lasers developed by our group. Although small variations of cavity length should compensate for each other in an ideal situation, there are usually small noneciprocal effects that cause backscatter to change and the beat note of the gyroscope to walk off from its nominal frequency [11,12].

For single-mode operation in a ring configuration, the coating is optimized for operation at a 45° angle of incidence with a designed transmission of 1.7 and 13.6 ppm for s- and p-polarized light, respectively. In detail, the high-reflectivity multilayer consists of 38.5 periods of alternating GaAs (high index, 3.45 at 1.152 μm, 85.5 nm ideal quarter-wave thickness) and $Al_{0.92}Ga_{0.08}As$ (low index, 2.96 at 1.152 μm, 99.5 nm ideal quarter-wave thickness). Spectrophotometer measurements of the as-grown epitaxial films reveal a very small thickness error of approximately −0.5%. The resulting 5.5 nm blue shift in the center wavelength of the high-reflectivity stopband to 1.1445 μm yields transmission values of 1.9 ppm (s) and 15.1 ppm (p) in the final optics at 1.152 μm. Optical absorption in the coating was independently probed on wafer at 1.155 μm via photothermal common path interferometry [13]. Because of significant loss within the optical path from water vapor in the ambient laboratory environment (on the order of 15 ppm/cm), these measurements can only provide an upper limit of 5 ppm, though there is evidence that the absorption loss for these specific coatings is at the 1 ppm level. At this early stage of development, scatter remains the biggest limitation in terms of optical performance for the crystalline supermirrors. The micro-roughness of the multilayer was investigated via atomic force microscopy and yielded an RMS value of 1.7 Å. In addition to the limiting micro-roughness, growth related defects dominate the overall scatter losses in this experiment. These defects are known to occur in MBE-grown GaAs films and work is currently under way to mitigate their presence. For the employed coatings, we observe 10 μm sized scattering centers with a density on the order of 1000 cm^{-2}, while defect densities as low as 10 cm^{-2} have been achieved in other instances. Note also that the large optical beam diameter of 3.67 mm in this experiment significantly increases the impact of scattering when compared with a diameter of 0.5 mm with the previously constructed linear reference cavity at 1.064 μm, where total scatter losses below 5 ppm have been observed. Using a simple exponential model [14] and ignoring interfacial or interference effects within the Bragg stack yields a lower limit of 3.4 ppm for the optical scatter at the operating wavelength of 1.152 μm, which is comparable to state-of-the-art ion beam sputtered supermirror coatings.

Employing these novel coatings, we present the results of experiments using a large helium–neon based ring laser operating in the near infrared. We have performed our experiments on a vertically (wall) mounted, 6.4 m perimeter square ring laser located in a second floor laboratory of a high rise building on the Ilam campus of the University of Canterbury in Christchurch, New Zealand. The cavity is entirely filled with helium–neon gas, and the only intra-avity elements are the spherical supermirrors. Radio frequency excitation of the gain medium at 80 MHz occurs within a narrow pyrex plasma tube of 4 mm diameter, thereby avoiding Langmuir flow. Operation on a single longitudinal mode is achieved through gain starvation with servo control of the rf power, maintaining a stable laser output. As expected, the crystalline mirrors only supported s-polarization in the laser cavity. A peltier cooled InGaAs detector was used to measure the combined output beams of the laser, which was performed using a short beam path in open air. The beam combiner itself was aligned using the residual sensitivity of Si-based CCD cameras at the laser wavelength, as well as standard hand-held IR viewers. The ring was first filled with a 50:50 mixture of Ne^{20} and Ne^{22}. Simultaneous laser oscillation was then observed on the well-known neon doublet split by 51 GHz ($2s_2 \rightarrow 2p_4$ at 1.152276 μm and $2s_4 \rightarrow 2p_7$ at 1.152502 μm) [15]. By varying the total pressure of this mixture and the rf excitation power, the regime of maximum gain was identified at a pressure of 0.2 hPa. Figure 2(a) shows the dependence of the laser gain over the total gas pressure in the cavity.

A ringdown measurement of the cavity provided a value of $\tau = 20$ μs, corresponding to a quality factor of

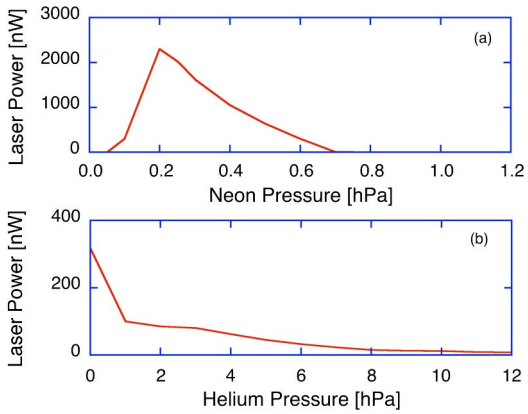

Fig. 2. Maximum obtainable laser power from pure neon as a function of total gas pressure (a). Gyroscope operation was possible in the regime between 1 and 10 hPa (b) when the laser gain from the rf excitation was reduced.

$Q = 2\pi\nu\tau = 3.2 \times 10^{10}$ with ν the oscillation frequency of the laser cavity. Thus, the total loss (L) of the cavity with a free spectral range (FSR) of 46.875 MHz amounts to $L = 1/(\tau \times \mathrm{FSR}) = 0.0011$. Similar seemingly high loss has been observed previously in many of our large ring lasers [4] and speculatively attributed to "waviness" in the mirror profiles. In this case, there is additional loss because of beam clipping, where light is transmitted past the edges of the reflective coatings. The total loss is a subject of ongoing investigation. With the application of a spatial filter blocking the spilled light, we estimate that this extra light leakage is about four times larger than the light loss from the transmission through the mirrors. Of course, one must bear in mind that the center of the TEM_{00} mode was attenuated by a factor of approximately 10^6 by the high-reflectivity coatings. Beam clipping losses can be easily remedied in future experiments as crystalline coatings of approximately 20 mm diameter have already been demonstrated in the context of the development of low-noise optics for interferometric gravitational wave detectors [16]. In a second step, ^{4}He was slowly added and the achievable laser power for a constant rf excitation of 8 W was measured. This is shown in Fig. 2(b). With only a small fraction of helium added, a significant drop in beam power was observed. This is attributable to the fact that helium efficiently quenches the 1.152502 μm transition through an increase in the $2p_7$ population [15].

Compared with the operation of the same cavity on a single longitudinal laser mode at a wavelength of 632.8 nm, the circulating laser power was considerably smaller. It required approximately 0.6 W of rf power to achieve 4.7 nW of output power, corresponding to 2.6 mW of intracavity laser power. In the visible, the same system operates at 2.5 W of rf providing 12 nW of optical power corresponding to 60 mW of intracavity beam power. It was also found that the multimode threshold is much closer to the monomode threshold in the infrared as opposed to the visible. Furthermore, it appears that increasing the gas pressure in the cavity does not enlarge the separation between the multimode threshold and the monomode threshold via homogeneous line broadening for operation at 1.152276 μm, whereas for operation on the 632.8 nm transition this has a considerable influence. Additionally, we observed a significant imbalance in beam power between the clockwise and counter-clockwise beams of about 15%, which is about a factor of 2 larger then routinely observed with ion beam sputtered mirrors.

Despite the comparatively low cavity Q, the laser operated as a gyroscope, unlocking on the rate bias provided by the earth rotation alone. To the best of our knowledge, this is the first time this has been reported in the literature. While the operation on a pure neon gas mix was helpful to align the laser properly by providing a brighter beam, it was of no use with respect to the operation as a gyroscope because of the presence of a highly variable additional beat note when simultaneous laser oscillation on both neon lines was observed. We reasonably attribute this phenomenon to mode competition. Since helium efficiently quenches the 1.152502 μm transition, the 1.152276 μm transition is the only remaining optical frequency and the gyroscope turned out to be operable as a rotation sensing device over the range of 1–10 hPa of helium.

Modulations are observed on the clockwise and counterclockwise beams at the Sagnac frequency given by Eq. (1), with fractional amplitudes m_1, m_2 which vary, but are typically 5%–8%. These modulations allow estimates of backscatter fractional amplitude coupling $r_{1,2}$ using $r_{1,2} = m_{1,2}\pi\delta f P/c$, with δf and P as in Eq. (1) [17]. In our case, amplitude couplings in the order 0.2–0.3 ppm are indicated. The expected backscatter induced perturbations are of the order $m_1 m_2 \delta f/2$ [17], in our case 0.1–0.2 Hz. The total fractional scattered intensity may be estimated as $r_s^2 \approx r^2 16d^2/\lambda^2$ [18] for beam diameter d. With $d = 3.6$ mm this gives ≈10 ppm. As this is the estimated scattering from four mirrors, it is in fairly good accord with the earlier estimated 3.4 ppm for a single mirror. The rotation rate threshold for lock-in of a ring laser gyro may be estimated as $\Omega_L = c\lambda^2 r_s/(32\pi A d)$ [18] for laser area A (with other symbols already defined). In our case, it is calculated as 1.4×10^{-6} rad/s which is ≈3% of the projected earth rotation rate. Thus, the observed absence of lock-in is expected.

Figure 3 shows a timeseries of about 45 min of the measurement of the earth's rotation as one example. Neither the laboratory nor the stainless steel ring laser structure was temperature stabilized; therefore, the data in the plot is highpass filtered to remove sensor drift. Apart from the earth's rotation, the measured rotation signal also shows a 2.36 Hz frequency modulation caused by the fundamental rocking mode of the entire eight floor Rutherford building about its long axis in the form of a small oscillation about the mean of the beat note. The frequency splitting of the two counter propagating laser beams according to Eq. (1) was measured to be 59 ± 2 Hz. With the latitude of the laboratory at 43.52° south, the vertical orientation of the ring laser structure on the laboratory wall and an orientation of the short side of the building of about 32° east of north, the expected Sagnac frequency according to Eq. (1) is around 60 Hz. In the presence of backscatter coupling from a concomitant frequency pulling, the observed data is in good agreement with expectation. Figure 4 shows the corresponding spectrum of the interferogram. The main beat note induced by earth's rotation shows the two sidebands induced by the rocking

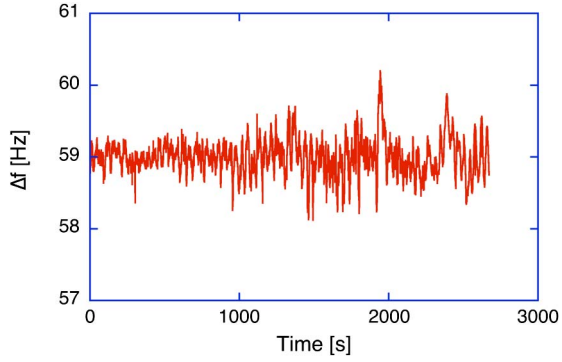

Fig. 3. Sagnac beat note from the earth's rotation, detected at a wavelength of $\lambda = 1.152$ μm. The observation was highpass filtered to compensate for variations caused by backscatter pulling.

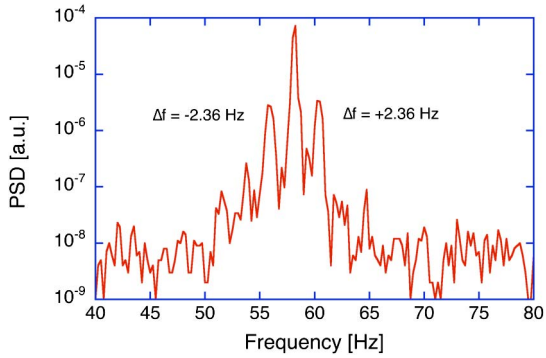

Fig. 4. Spectrum of the measured rotational signal shows the earth's rotation as the dominant signal, together with frequency modulation sidebands induced by the rocking of the building.

motion of the building at 2.36 Hz separation on either side of the main peak.

In summary, we have successfully obtained unlocked rotation sensing of a large HeNe ring laser gyroscope in the infrared regime rate biased by the earth's rotation alone. Moreover, we observe encouraging performance for the first implementation of crystalline coatings in an active laser cavity. Future work will focus on improvements in the overall system, as well as on the ultimate optical and thermo-mechanical performance of crystalline supermirrors and their impact on large-area and high-sensitivity RLGs.

The authors acknowledge support from the German national science foundation DFG under contract Schr645/6-1 and assistance from the Marsden Fund of the Royal Society of New Zealand under contract 10-UOC-041. G. D. Cole acknowledges support from EURAMET/EMRP (QESOCAS) and thanks Dr. A. Alexandrovski of SPTS for performing optical absorption measurements. A portion of this work was performed in the UCSB Nanofabrication Facility.

References

1. W. M. Macek and D. T. M. Davies, Jr., App. Phys. Lett. **2**, 67 (1963).
2. A. Javan, W. R. Bennett, Jr., and D. R. Herriott, Phys. Rev. Lett. **6**, 106 (1961).
3. K. U. Schreiber and J.-P. R. Wells, Rev. Sci. Instrum. **84**, 041101 (2013).
4. R. B. Hurst, G. E. Stedman, K. U. Schreiber, R. J. Thirkettle, R. D. Graham, N. Rabeendran, and J.-P. R. Wells, J. Appl. Phys. **105**, 113115 (2009).
5. S. F. Jacobs and R. Zanoni, Am. J. Phys. **50**, 659 (1982).
6. R. B. Hurst, J.-P. R. Wells, and G. E. Stedman, J. Opt. A **9**, 838 (2007).
7. K. U. Schreiber, T. Klügel, A. Velikoseltsev, W. Schlüter, G. E. Stedman, and J.-P. R. Wells, Pure Appl. Geophys. **166**, 1485 (2009).
8. N. Beverini, M. Allegrini, A. Beghi, J. Belfi, B. Bouhadef, M. Calamai, G. Carelli, D. Cuccato, A. Di Virgilio, E. Maccioni, A. Ortolan, A. Porzio, R. Santagata, S. Solimeno, and A. Tartaglia, Laser Phys. **24**, 074005 (2014).
9. Y. B. Band, *Light and Matter* (Wiley, 2006), p. 187.
10. G. D. Cole, W. Zhang, J. Ye, and M. Aspelmeyer, Nat. Photonics **7**, 644 (2013).
11. R. W. Dunn and A. R. Hosman, J. Appl. Phys. **116**, 173109 (2014).
12. R. Rodloff, IEEE J. Quantum Electron. **23**, 438 (1987).
13. A. Alexandrovski, M. Fejer, A. Markosian, and R. Route, Proc. SPIE **7193**, 71930D (2009).
14. H. Davies, Proc. IEEE **101**, 209 (1954).
15. W. R. Bennett, Jr. and J. W. Knutson, Jr., Proc. IEEE **52**, 861 (1964).
16. J. Steinlechner, I. W. Martin, A. Bell, G. Cole, J. Hough, S. Penn, S. Rowan, and S. Steinlechner, "Mapping the Optical Absorption of a Substrate-Transferred Crystalline AlGaAs Coating at 1.5 μm," December 2014, http://arxiv.org/abs/1412.3627.
17. R. B. Hurst, N. Rabeendran, K. U. Schreiber, and J.-P. R. Wells, Appl. Opt. **53**, 7610 (2014).
18. F. Aronowitz, *Laser Applications*, M. Ross, ed. (Academic, 1971), Vol. **I**, p. 133